MISSOURI S&T

Missouri University of Science and Technology
Scholars' Mine

International Specialty Conference on Cold-Formed Steel Structures

(1971) - 1st International Specialty Conference on Cold-Formed Steel Structures

Aug 20th

Inelastic Buckling of Thin-Walled Members

S. Rajasekaran

D. W. Murray

Follow this and additional works at: http://scholarsmine.mst.edu/isccss

 Part of the Structural Engineering Commons

Recommended Citation

Rajasekaran, S. and Murray, D. W., "Inelastic Buckling of Thin-Walled Members" (1971). *International Specialty Conference on Cold-Formed Steel Structures*. 3.
http://scholarsmine.mst.edu/isccss/1iccfss/1iccfss-session2/3

This Article - Conference proceedings is brought to you for free and open access by Scholars' Mine. It has been accepted for inclusion in International Specialty Conference on Cold-Formed Steel Structures by an authorized administrator of Scholars' Mine. This work is protected by U. S. Copyright Law. Unauthorized use including reproduction for redistribution requires the permission of the copyright holder. For more information, please contact scholarsmine@mst.edu.

INELASTIC BUCKLING OF THIN-WALLED MEMBERS

by S. Rajasekaran[1] and D.W. Murray[2]

INTRODUCTION

The use of light gage steel, and slender members of open cross section, in cold-formed construction, makes it desirable to have a knowledge of critical member loading and post-buckling behavior in order to devise safe and economical design procedures. Except for very slender members, some inelastic behavior usually occurs prior to the attainment of maximum load carrying capacity. There is, therefore, a need to study the problem of the determination of critical loading for inelastic members.

Inelastic lateral and lateral torsional buckling have been investigated by Galambos (6,7) and others (10). Since a comprehensive closed form solution is not available, and is unlikely to be forthcoming, a flexible general purpose numerical approach would be of value. The object of this paper is to present a finite-element formulation to determine critical (bifurcation)loading conditions on a member of thin-walled open cross-section, including the effects of inelastic material response, for any arbitrary statically determinate loading. The analysis includes the effect of residual stress but neglects the effect of prebuckling displacements on the equilibrium equations.

BASIC ASSUMPTIONS

The assumptions used in this formulation are consistent with those used in classical inelastic buckling analysis of columns (4,15). It is assumed that a reasonable estimate of the maximum load carrying capacity may be obtained by employing Shanley's tangent modulus concepts (14). The basic assumption is that no strain reversal occurs, and therefore the effective incremental stiffness at any section may be determined from the instantaneous tangent modulus values at all parts of the cross-section. Since the stress in the member is essentially uniaxial, the effective strain for the determination of tangent moduli is considered to be the longitudinal strain. The incremental section properties may then be computed by a transformed area concept.

In addition, the following assumptions have been made:

(1) Members are initially straight and prismatic.
(2) The projection of the cross-section on a plane normal to the centroidal axis does not distort.
(3) Displacements of a point may be obtained by superimposing warping displacements on plane section displacements, each of which are consistent with simple beam theory (12, 15, 16).
(4) The residual stress distribution satisfies statics.
(5) Variation of longitudinal stress across the plate thickness may be neglected.
(6) The effect of prebuckling displacements on the equilibrium equations may be neglected.
(7) Boundary conditions are such that the structure remains statically determinate.
(8) The stress-strain curve is tri-linear (Fig. 1).

[1]Graduate Student, University of Alberta, Edmonton, Alberta.

[2]Professor of Civil Engineering, University of Alberta, Edmonton, Alberta,

It should be noted that it is by virtue of assumptions (1) and (6) that the more realistic, but numerically more difficult, beam-column problem is converted to a bifurcation problem.

GOVERNING EQUATIONS

An incremental equilibrium equation, derived from the principle of virtual work and thus valid for any constitutive relation, may be expressed in variational form as (13).

$$\frac{1}{2}\int_V \bar{\sigma}_{ij}\,\delta(u_{k,i}u_{k,j})dV + \frac{1}{2}\int_V \sigma_{ij}\,\delta(u_{i,j}+u_{j,i}+u_{k,i}u_{k,j})dV$$

$$+\frac{1}{2}\int_V \sigma_{ij}\,\delta(\bar{u}_{k,i}u_{k,j}+u_{k,i}\bar{u}_{k,j})dV = \int_S t_i\,\delta u_i\,ds \qquad (1)$$

where t_i = increments in surface tractions, u_i = increments in the displacement vector, σ_{ij} = the increment of the stress tensor, $\bar{u}_k$ = the displacement vector prior to the increment, $\bar{\sigma}_{ij}$ = the stress tensor prior to the increment, and V and S are the volume and surface of the member, respectively.

By assuming the initial displacements, $\bar{u}_k$, are negligible (see assumption (6)); neglecting the displacement products in the second integral; expressing the displacements in terms of those at arbitrary reference axes (see Fig. 2) according to the standard beam assumptions (see assumption (3)); and integrating over the area; the incremental equilibrium Eq. 1 may be expressed in terms of stress resultants, increments in stress resultants and variations in displacements, as (13).

$$\int_L \{\Delta P\,\delta w_c' - \Delta M_x\,\delta v_s'' - \Delta M_y\,\delta u_s'' + \Delta W_w\,\delta\phi'' + V_x\phi\,\delta v_s'$$

$$+ V_x v_s'\,\delta\phi - V_y\phi\,\delta u_s' - V_y u_s'\,\delta\phi + P u_s'\,\delta u_s' + P v_s'\,\delta v_s'$$

$$+ P e_y u_s'\,\delta\phi' + P e_y \phi'\,\delta u_s' - P e_x v_s'\,\delta\phi' - P e_x \phi'\,\delta v_s'$$

$$- M_x u_s'\,\delta\phi' + M_y v_s'\,\delta\phi' - M_x \phi'\,\delta u_s' + M_y \phi'\,\delta v_s' + M_\rho \phi'\,\delta\phi'$$

$$+ T_{sv}\,\delta\phi' - (\Delta q_x\,\delta u_s + \Delta q_y\,\delta v_s + \Delta q_z\,\delta w_z + \Delta m_t\,\delta\phi + \Delta m_x\,\delta v_s'$$

$$+ \Delta m_y\,\delta u_s')\,dz = 0 \qquad (2)$$

where (') indicates differentiation with respect to z; displacements and co-ordinates are illustrated in Fig. 2; P, V_x, V_y, M_x, M_y = the usual stress resultants (Fig. 2); M_ρ and T_{sv} are stress resultants defined in Appendix II - Notation; and q_x, q_y, q_z, m_x, m_y, m_t = distributed loads and couples per unit of length, respectively.

Integrating by parts leads to the Euler - Lagrange equilibrium equations of a beam-column

$$\frac{dP}{dz} + q_z = 0 \qquad (3\text{-a})$$

$$(M_y)'' - (M_x\phi)'' + (Pu_s')' + (Pe_y\phi')' + q_x - m_y' = 0 \qquad (3\text{-b})$$

$$(M_x)'' + (M_y\phi)'' + (Pv_s')' - (Pe_x\phi')' + q_y - m_x' = 0 \qquad (3\text{-c})$$

$$W_w'' + M_x u_s'' - M_y v_s'' - (M_\rho\phi')' - (Pe_y u_s')' + (Pe_x v_s')'$$

$$- m_t - T_{sv}' = 0 \qquad (3\text{-d})$$

which are identical with Vlassov's (16) equations if the section remains elastic.

The finite element formulation seeks to establish numerical approximations for the displacements which satisfy the equilibrium Eqs. 3, by substituting assumed forms of displacements into the equivalent virtual work expression, Eq. 2. The total virtual work may be evaluated by summing

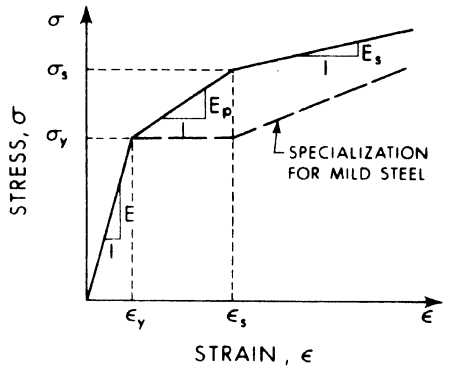

FIG. 1 Tri-Linear Stress-Strain Diagram

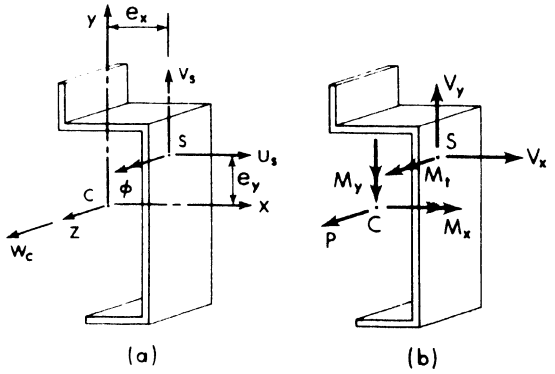

FIG. 2 Reference Axes, Displacements and Stress Resultants

the integrals over each element, and the reference axes in each element may be different providing the displacement variations are compatible at the junction of any two elements.

Equation 2 may therefore be written as

$$\sum_{1}^{M}\left\{\int_{\ell_m}\left[\Delta P\,\delta w_\zeta' - \Delta M_\xi\,\delta v_\eta'' - \Delta M_\eta\,\delta u_\xi'' + \Delta W_{w\zeta}\,\delta\phi'' + V_\xi v_\eta'\,\delta\phi\right.\right.$$

$$+ V_\xi\phi\,\delta v_\eta' - V_\eta\phi u_\xi' - V_\eta u_\xi'\,\delta\phi + Pu_\xi'\,\delta u_\xi' + Pv_\eta'\,\delta v_\eta'$$

$$+ Pe_\eta u_\xi'\,\delta\phi' + Pe_\eta\,\phi'\,\delta u_\xi' - Pe_\xi v_\eta'\,\delta\phi' - Pe_\xi\phi'\delta v_\eta'$$

$$- M_\xi u_\xi'\,\delta\phi' + M_\eta v_\eta'\,\delta\phi' - M_\xi\phi'\,\delta u_\xi' + M_\eta\phi'\,\delta v_\eta'$$

$$\left.\left. + M_{\rho\zeta}\phi'\,\delta\phi' + T_{sv}\,\delta\phi' - (\Delta q_\xi\,\delta u_\xi + \Delta q_\eta\,\delta v_\eta + \Delta q_\zeta\,\delta w_\zeta\right.\right.$$

$$\left.\left. + \Delta m_\zeta\,\delta\phi + \Delta m_\xi\,\delta v_\eta' + \Delta m_\eta\,\delta u_\xi')\right]\,d\zeta\right\} = 0 \qquad (4)$$

where M = the number of elements; $\bar{C}$ and $\bar{S}$ = the centroid and shear center of the transformed partially yielded section; ξ and η = the transformed section principal axes; and stress resultant increments, displacements and co-ordinate relationships are shown in Figs. 3 and 4.

The stress resultant increments appearing in Eq. 4 may be written in the following uncoupled form:

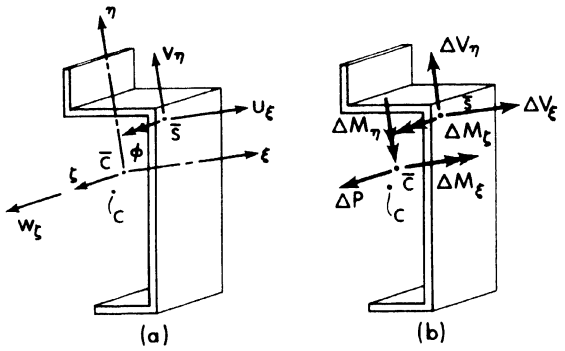

FIG. 3 Transformed Section Axes, Displacements and Stress Resultant Increments

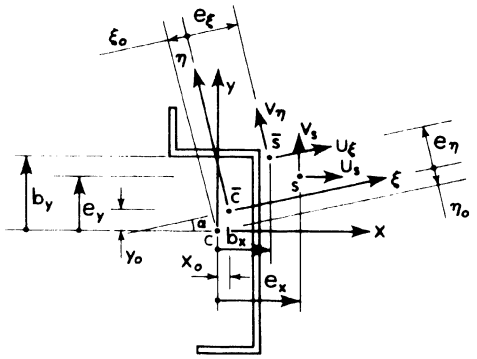

FIG. 4 Displacement Transformation

$$\Delta P = EA^T w_\zeta' \qquad (5\text{-a})$$

$$\Delta M_\xi = -EI_\xi^T v_\eta'' \qquad (5\text{-b})$$

$$\Delta M_\eta = -EI_\eta^T u_\xi'' \qquad (5\text{-c})$$

$$\Delta W_{w\zeta} = EI_{w\zeta}^T \phi'' \qquad (5\text{-d})$$

where A^T, I_ξ^T, I_η^T, and $I_{w\zeta}^T$ are properties of the transformed section, for which expressions are derived in Appendix IV - Section Properties.

The total stress resultants appearing in Eq. 4 need not be expressed in terms of displacements and may be evaluated by direct integration of the stresses as detailed in Appendix V - Stress Resultants.

FINITE ELEMENT IDEALIZATION

The finite element model used in this analysis employs cubic displacement functions to represent u_ξ, v_η, and ϕ, and a quadratic dis-

placement function to represent w_ζ. It is interesting to note that the linear displacement function for w, used by other investigators (see, for example, Barsoum and Gallagher(1,2)) is inadequate to achieve a balance of axial forces for nonuniform inelastic response.

The displacements in Eq. 4 are therefore approximated, in a finite element segment, by

$$u_\xi = < f_3 > \{\underline{u}\} \tag{6-a}$$

$$v_\eta = < f_3 > \{\underline{v}\} \tag{6-b}$$

$$\phi = < f_3 > \{\underline{\phi}\} \tag{6-c}$$

$$w_\zeta = < f_2 > \{\underline{w}\} \tag{6-d}$$

where

$$< f_3 > = < (1 - 3\beta^2 + 2\beta^3),\ (\beta - 2\beta^2 + \beta^3),\ (3\beta^2 - 2\beta^3),\ (\beta^3 - \beta^2) > \tag{7-a}$$

and

$$< f_2 > = < (2\beta - 1)(\beta - 1),\ -4\beta(\beta - 1),\ \beta(2\beta - 1) > \tag{7-b}$$

The nondimensional co-ordinate, β, and the nodal vectors $\{\underline{u}\}$, $\{\underline{v}\}$, $\{\underline{\phi}\}$, and $\{\underline{w}\}$ are defined in Fig. 5.

Assuming that the section properties of Eq. 5 vary linearly along the length of the element; that the stress resultants prior to the load increment also vary linearly; and using Eqs. 5, 6, and 7 to evaluate the contribution of one element to Eq. 4, yields an algebraic set of element equilibrium equations, which may be written symbollically as

$$[\bar{k}_s]\{\bar{\Delta}r_E\} + [\bar{k}_G]\{\bar{\Delta}r_E\} = \{\bar{\Delta}R_E\} \tag{8}$$

where the element matrices are derived in Appendix VI - Element Matrices; and $\{\bar{\Delta}r_E\}$ and $\{\bar{\Delta}R_E\}$ = the vector of element nodal displacement increments and element nodal load increments, respectively, associated with transformed section axes.

Expressing the transformed section nodal displacement increments in terms of nodal displacement increments associated with the original reference axes, $\{\Delta r_E\}$, by the transformation

$$\{\bar{\Delta}r_E\} = [T]\{\Delta r_E\} \tag{9}$$

; premultiplying by $[T]^T$, the associated force transformation; and assembling by the direct stiffness method, yields the set of equations

$$[K_s]\{\Delta r\} + [K_G]\{\Delta r\} = \{\Delta R\} \tag{10}$$

where $\{\Delta r\}$ and $\{\Delta R\}$ = the assembled vectors of nodal displacement increments and force increments, respectively; and $[K_s]$ and $[K_G]$ are referred to as the 'tangent stiffness' and 'geometric stiffness', respectively. The basis for the transformation matrix [T] is developed in Appendix VI - Element Matrices.

SOLUTION PROCEDURE

A bifurcation loading condition has been attained if it is possible to determine nontrivial solutions to Eq. 10, for $\{\Delta R\} = 0$.

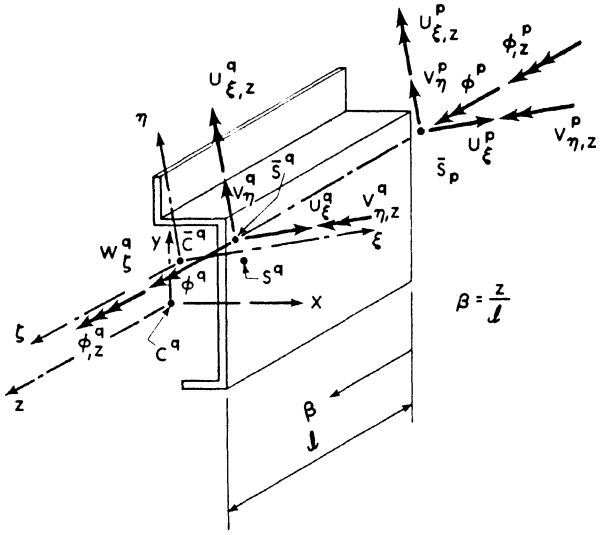

$$\{\underline{u}\}^T = <u_\xi^p,\ \ell u_{\xi,z}^p,\ u_\xi^q,\ \ell u_{\xi,z}^q>$$

$$\{\underline{v}\}^T = <v_\eta^p,\ \ell v_{\eta,z}^p,\ v_\eta^q,\ \ell v_{\eta,z}^q>$$

$$\{\underline{\phi}\}^T = <\phi^p,\ \ell\phi^p{}_{,z},\ \phi^q,\ \ell\phi^q{}_{,z}>$$

$$\{\underline{w}\}^T = <w_\zeta^p,\ w_\zeta^{(p+q)/2},\ w_\zeta^q>$$

FIG. 5 Element Nodal Parameters

The condition required to satisfy this requirement is that the determinant of the coefficient matrix be equal to zero, i.e.:

$$\det([K_s] + [K_G]) = 0 \tag{11}$$

If $[K_s]$ were independent of load and $[K_G]$ were linearly dependent on load, the critical loading could be obtained from a standard eigenvalue analysis. However, for an arbitrary cross section, subjected to arbitrary loads, the matrix $[K_s]$ is highly sensitive to the loading condition after inelastic response has been initiated.

The critical loading may now be determined in a number of ways. Fukumoto (5,6) has evaluated the determinant and extrapolated or interpolated this value to determine the loading for which Eq. 11 is satisfied. Harris and Pifko (9) have used an iterative approach on the load and found the load level for which the eigenvalue was one. The approach which the authors have used is to iterate for an eigenvalue to determine critical length rather than critical load. The procedure is described below.

For any arbitrary statically determinate loading, equilibrium is established, including the effects of inelastic material response but neglecting the effect of displacements on the equilibrium equations, by an iterative procedure detailed in Appendix III. Knowing the strains throughout the member, the tangent stiffness matrix $[K_s]$ can be established as outlined in the previous section and detailed in Appendices IV and VI. The prebuckling stress resultants can also be established by simple integration as detailed in Appendix V. This permits the evaluation of $[K_G]$

as detailed in Appendix VI.

An examination of the element and transformation matrices in Appendix VI shows that Eq. 10 may be written as

$$[[K_1] + [K_2] + [K_3]]\ \{\Delta r\} + [K_G]\ \{\Delta r\} = \{\Delta R\} \tag{12}$$

where K_1, K_2, and K_3 contain terms dependent on the inverse of ℓ, ℓ^2, and ℓ^3, respectively. Noting that $[K_G]$ is proportional to the inverse of ℓ; defining the critical element length, ℓ_c, as $\ell_c = \lambda\ell$, and factoring λ; the condition for the existence of nontrivial solutions of Eq. 12 with $\{\Delta R\} = 0$ may be written as

$$\frac{1}{\lambda^2}\ [[K_3] + \lambda[K_2] + \lambda^2[K_1]]\{\Delta r\} = -\ [K_G]\{\Delta r\} \tag{13}$$

This equation may be abbreviated as

$$\frac{1}{\lambda_{i+1}^2}\ [K(\lambda_i)]\{\Delta r\} = -[K_G]\ \{\Delta r\} \tag{14}$$

Assuming a value for λ_i, an eigenvalue solution will yield λ_{i+1}. Equation 14 may be iterated until $\lambda_{i+1} = \lambda_i$, at which time the critical length has been determined. For practical purposes the first iterate is usually sufficient.

It should be noted that the above procedure is only valid if the stress resultants remain constant at each node as the member length is scaled. A simultaneous scaling of the transverse loading is therefore required to satisfy this condition. Since stress resultants are not proportional to loading for statically indeterminate inelastic structures, the method is applicable only to statically determinate structures.

NUMERICAL SOLUTIONS

Fig. 6 shows a comparison of critical σ/σ_y versus L/r ratios, obtained from this analysis, with previously published results for a double angle section subjected to axial compression. For the section chosen the elastic analysis yields essentially the same results for lateral torsional and weak axis buckling, and hence only one has been plotted. Nuttal's solution (11) was obtained by imposing a uniform axial strain, evaluating transformed section properties numerically and solving the normal stability equations for the critical length. The influence of residual stress and the significance of inelastic response is apparent.

Fig. 7 shows a comparison of the nondimensionalized critical moment versus L/r ratio for an 8WF 31 subjected to a constant moment. A solution of this problem was obtained by Galambos (8). The importance of residual stress is again demonstrated and the comparison is reasonably good.

Fig. 8 compares the critical uniform moment required to produce inelastic lateral torsional buckling of an 8 WF 31, subjected to constant axial load, to that obtained by Galambos (7). The comparison is again considered reasonable.

Fig. 9 compares the critical end moment required to produce lateral torsional buckling of an 8 WF 31, subjected to a constant axial load to that obtained by Fukumoto (5,6). In contrast to the preceding solutions, Fukumoto's solution includes the effect of in-plane prebuckling displacements in arriving at an equilibrium configuration. The critical load is then determined as that for which the determinant vanishes. The effect of prebuckling displacements is apparently small.

Fig. 10 shows the results obtained when a 14 WF 43 section is subjected to biaxial bending produced by a doubly eccentric axial load. Results are presented with and without residual stress. The finite element solution of the inelastic beam-column problem was also obtained for three L/r ratios. The effect of prebuckling displacements and residual stress is apparent. The location of point A is consistent with the results of Birnstiel (3).

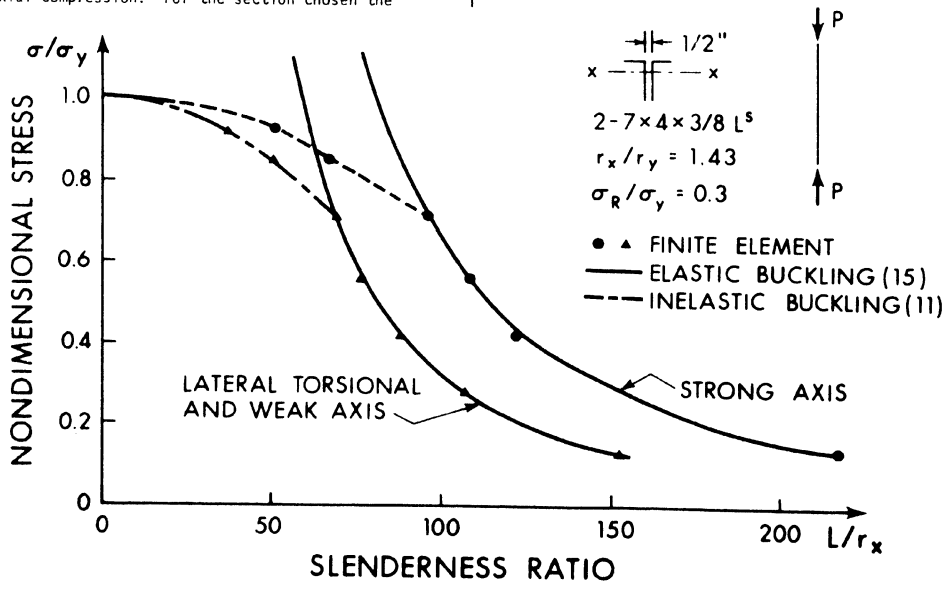

FIG. 6 Inelastic Buckling of Double Angle Strut

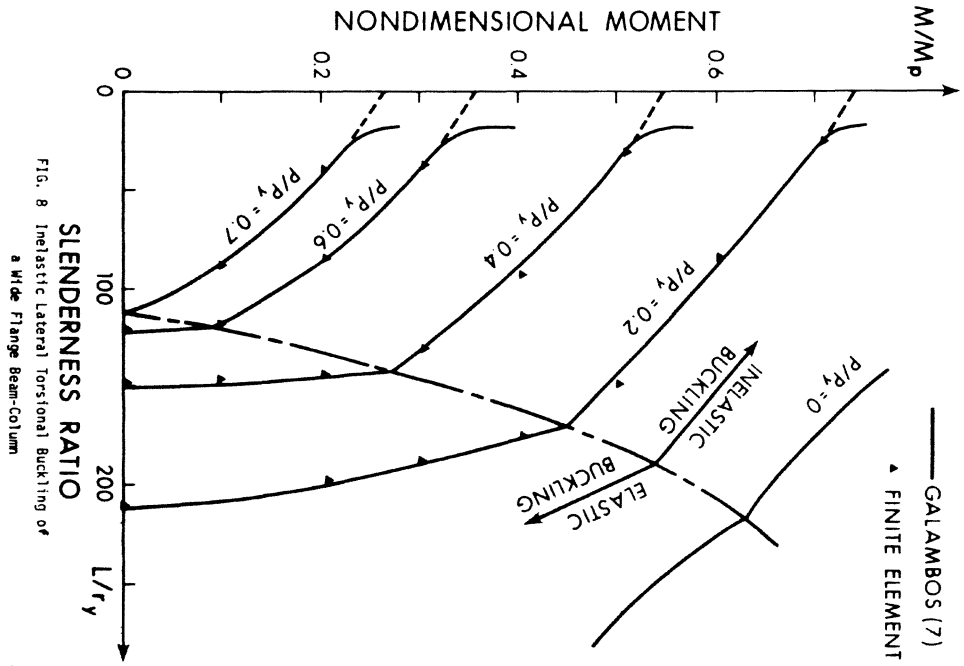

FIG. 8 Inelastic Lateral Torsional Buckling of a Wide Flange Beam-Column

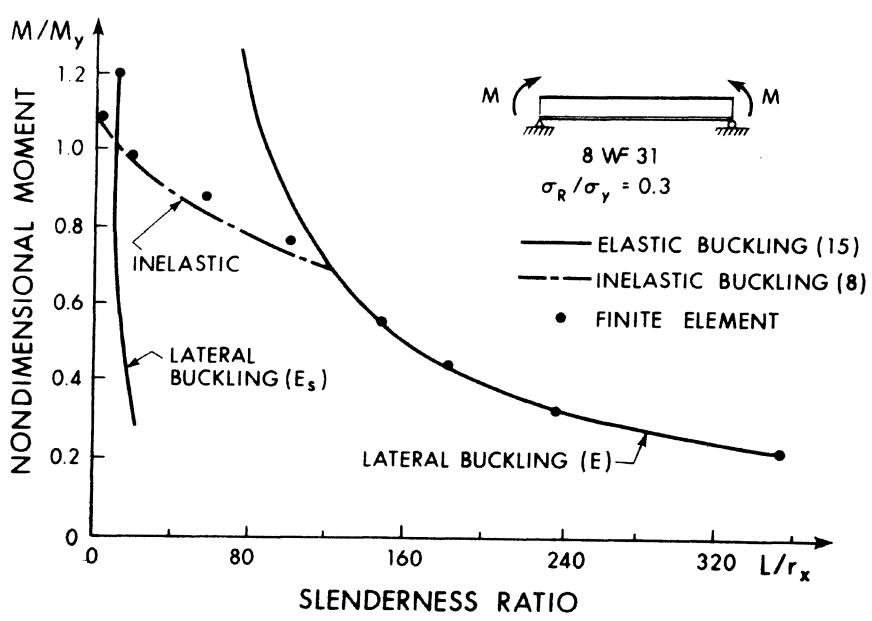

FIG. 7 Inelastic Lateral Buckling of a Wide Flange Beam

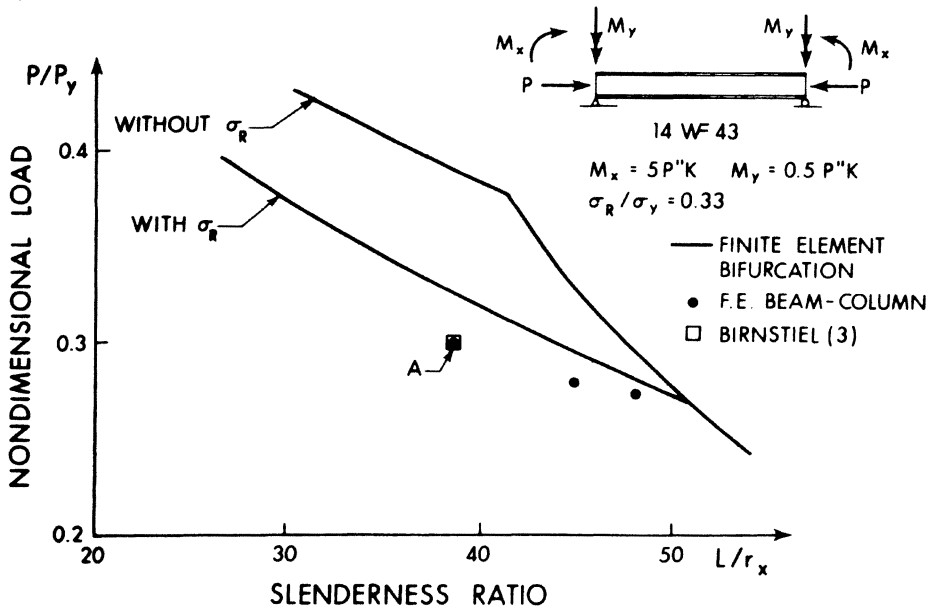

FIG. 10 Inelastic Buckling for Biaxial Bending with Axial Load

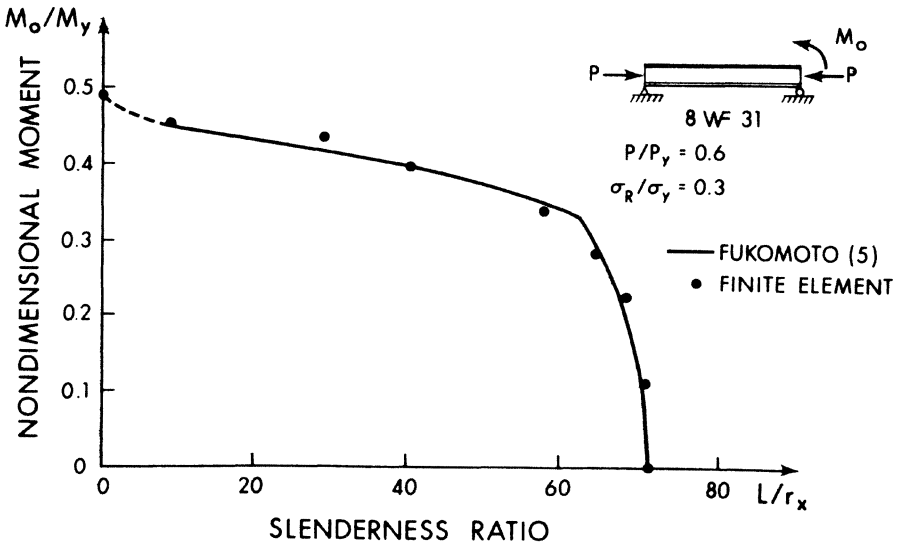

FIG. 9 Inelastic Lateral Torsional Buckling of a Beam-Column with Moment Gradient

SUMMARY AND CONCLUSIONS

A general purpose finite element program has been developed to determine the inelastic buckling strength of thin-walled prismatic members, with arbitrarily shaped open cross-sections, for any statically determinate loading condition, with a trilinear stress-strain response curve, and including the effects of residual stress. The analysis is capable of predicting lateral, torsional and lateral-torsional buckling modes, and yields reasonable results for a large class of problems.

The critical loads determined from the analysis represent upper bounds on load carrying capacities because the effects of prebuckling displacements have been neglected. When prebuckling displacements have a significant effect on load capacity it is necessary to solve the more complex nonlinear load-displacement problem, rather than the bifurcation problem. Such a situation is illustrated in Fig. 10. Work is presently underway on this class of problem.

APPENDIX I - REFERENCES

1. Barsoum, R.S., "A Finite Element Formulation for the General Stability Analysis of Thin-Walled Members," Ph.D. Dissertation, Cornell University, 1970.
2. Barsoum, R.S., and Gallagher, R.H., "Finite Element Analysis of Torsional and Torsional-Flexural Stability Problems," Int. J. for Numerical Methods in Engineering, Vol. 2, No. 1, 1970.
3. Birnstiel, C., "Experiments on H Columns under Biaxial Bending," Journal of the Structural Division, ASCE, Vol. 94, No. ST10, October 1968, pp. 2429-2449.
4. Bleich, F., "Buckling Strength of Metal Structures," McGraw-Hill Book Co., Inc., New York, 1952.
5. Fukumoto, Y., "Inelastic Lateral-Torsional Buckling of Beam Columns," Ph.D. Dissertation, Lehigh University, 1963.
6. Fukumoto, Y., and Galambos, T.V., "Inelastic Lateral-Torsional Buckling of Beam-Columns," Journal of the Structural Division, ASCE, Vol. 92, No. ST2, April 1966, pp. 41-61.
7. Galambos, T.V., "Inelastic Lateral-Torsional Buckling of Eccentrically Loaded Wide-Flange Columns," Ph.D. Dissertation, Lehigh University, 1959.
8. Galambos, T.V., "Inelastic Lateral Buckling of Beams," Journal of the Structural Division, ASCE, Vol. 89, No. ST5, October 1963, pp. 217-242.
9. Harris, H.G. and Pifko, A.B., "Elastic-Plastic Buckling of Stiffened Rectangular Plates," Proceedings of the Symposium on Application of Finite Element Methods in Civil Engineering, Nashville, Tennessee, November 1969.
10. Massey, C. and Pitman, F.S., "Inelastic Lateral Stability under a Moment Gradient," Journal of the Engineering Mechanics Division, ASCE, Vol. 92, No. EM2, April 1966, pp 101-111.
11. Nuttall, N.J. and Adams, P.F., "Flexural and Lateral Torsional Buckling Strength of Double Angle Struts," Structural Engineering Report No. 30, Department of Civil Engineering, University of Alberta, 1970.
12. Oden, J.T., "Mechanics of Elastic Structures," McGraw-Hill Book Co., Inc., 1967.
13. Rajasekaran, S., "Finite Element Analysis of Thin-Walled Members," Ph.D. Dissertation, University of Alberta, 1971.
14. Shanley, F.R., "Inelastic Column Theory," Journal of Aeronautical Sciences, Vol. 14, No. 5, May 1947.
15. Timoshenko, S.P. and Gere, J.M., "Theory of Elastic Stability," 2nd Edition, McGraw-Hill Book Co., Inc., New York, 1961.
16. Vlasov, V.Z., "Thin-Walled Elastic Beams," 2nd Edition, Israel Program for Scientific Translations, Jerusalem, 1961.

APPENDIX II - NOTATION

A = area; point on section (Fig. 12)

A^T = transformed area

b = plate segment length (Fig. 12)

C, $\bar{C}$ = centroid; transformed area centroid

e_x, e_y = shear center co-ordinates

E, E_p, E_s = elastic moduli (Fig. 1)

G = shear modulus

I_ξ^T, I_η^T = transformed section principal moments of inertia

I_w, $I_{w\zeta}$ = sectorial moment of inertia; transformed section sectorial moment of inertia

$J = \Sigma bt^3/3$ = St. Venant constant

k = plate segment index

$[\bar{k}_s]$, $[\bar{k}_G]$ = tangent and geometric element stiffness matrices

$[K_s]$, $[K_G]$ = tangent and geometric assembled stiffness matrices

M_x, M_y, M_ξ, M_η = moments about respective axes

$M_\rho = \int \sigma_z \rho^2 dA$ = a stress resultant

m_x, m_y, m_z = distributed couple loads

p, q = nodal numbers

q_x, q_y, q_z = distributed loads

r = plate region index

$\{r\}$, $\{\Delta r\}$ = assembled nodal displacement vector and its increment

$\{R\}$, $\{\Delta R\}$ = assembled nodal force vector and its increment

S = surface area; shear center

$\bar{S}$ = transformed section shear center

S_w, S_{wx}, S_{wy} = sectorial static moment and sectorial linear static moments about the x and y axes, respectively

t = plate thickness

t_i = surface traction increment

$T_{sv} = GJ\phi'$ = St. Venant torque

u_s, v_s, u_ξ, v_η = shear center displacements

V = volume

V_x, V_y, V_ξ, V_η = shear stress resultants

w_c = z displacement of C

W_w, $W_{w\zeta}$ = bimoments

x, y, z = centroidal axes

x_o, y_o = distances defined in Fig. 4

X_{ir}, Y_{ir} = region co-ordinates (Fig. 12)

α = rotation of axes (Fig. 4)

β = nondimensional co-ordinate (Fig. 5)

ϵ = strain

ϵ_y, ϵ_p = strains defined in Fig. 1

λ = eigenvalue

ϕ = angle of twist

$\bar{\sigma}_{ij}$, σ_{ij} = stress tensor and increment

σ_y, σ_s = stresses defined in Fig.1

ω = sectorial co-ordinate

$\bar{\omega}$ = normalized warping with pole $\bar{S}$

$\hat{\omega}$ = normalized warping with pole S

APPENDIX III -

ALGORITHM FOR DETERMINING INELASTIC CRITICAL LENGTHS

STEP 1. DETERMINE STATIC STRESS RESULTANTS

(a) Subdivide the member into elements of equal length.

(b) Compute the elastic section properties A, I_x, I_y, I_{xy}, K_T, I_w and $\hat{I}_x$ and $\hat{I}_y$, where

$$\hat{I}_x = I_x(1 - I_{xy}^2 / I_x I_y) \quad (15\text{-a})$$

$$\hat{I}_y = I_y(1 - I_{xy}^2 / I_x I_y) \quad (15\text{-b})$$

with C and S located at the centroid and shear centre of the section, (Fig. 2).

(c) Solve for displacements, with $[K_G] = 0$ and $[K_s]$ determined from elastic properties.

(d) Compute stress resultants $\hat{P}$, $\hat{M}_x$, $\hat{M}_y$ and $\hat{W}_w$ at each node for this small deflection solution.

NOTE: The stress resultants determined in this way are those which equilibrate the external forces.

STEP 2. DETERMINE STRAINS(ITERATIVELY)WHICH PRODUCE STATIC STRESS RESULTANTS

(a) Compute strains from the initial approximate displacements, as

$$\varepsilon = w_c' - y\, v_s'' - x\, u_s'' + \bar{\omega}\, \phi'' + \varepsilon_R \quad (16)$$

(b) Calculate stress resultants, P, M_x, M_y and W_w, (see Appendix V) for the given strain distribution.

(c) Compute the unbalance in stress resultants, as

$$\bar{P} = \hat{P} - P \quad (17\text{-a})$$

$$\bar{M}_x = \hat{M}_x - M_x \quad (17\text{-b})$$

$$\bar{M}_y = \hat{M}_y - M_y \quad (17\text{-c})$$

$$\bar{W}_w = \hat{W}_w - W_w \quad (17\text{-d})$$

(d) Compute equivalent unbalanced stress resultants, P^*, M_x^*, M_y^* and W_w^* about C and S, where

$$P^* = \bar{P} \quad (18\text{-a})$$

$$W_w^* = \bar{W}_w \quad (18\text{-b})$$

$$M_x^* = \bar{M}_x - \bar{M}_y\, I_{xy}/I_y \quad (18\text{-c})$$

$$M_y^* = \bar{M}_y - \bar{M}_x\, I_{xy}/I_x \quad (18\text{-d})$$

(e) Estimate strain increments, from the equation

$$\Delta\varepsilon_i = \frac{P^*}{A} + \frac{M_x^*}{\hat{I}_x} y + \frac{M_y^*}{\hat{I}_y} x + \frac{W_w^*}{I_w} \bar{\omega} \quad (19)$$

and a new approximate strain, as

$$\varepsilon_{i+1} = \varepsilon_i + \Delta\varepsilon_i \quad (20)$$

(f) Iterate on steps (2-b) to (2-e) until the unbalanced stress resultants are negligible.

NOTE: A set of strains have now been determined which will provide stress resultants to equilibrate the external forces, assuming the pre-buckling displacements have negligible effect on the equilibrium equations.

STEP 3. COMPUTATION OF TANGENT AND GEOMETRIC STIFFNESS MATRICES

(a) The tangent stiffness matrix, $[K_s]$, of Eq. 10 may now be evaluated as outlined in the paper and detailed in Appendices IV and VI.

(b) The geometric stiffness matrix, $[K_G]$, of Eq. 10 may now be evaluated as outlined in the paper and detailed in Appendices V and VI.

STEP 4. SOLUTION FOR CRITICAL LENGTH

(a) Eq. 14 is solved for λ, to determine the critical length $\ell_c = \lambda\ell$, as described in the solution procedure.

APPENDIX IV - SECTION PROPERTIES

The determination of stress resultant increments by Eqs. 5 requires the evaluation of the tangent modulus properties A^T, I_ξ^T, I_η^T, and $I_{w\zeta}^T$. This may be accomplished as follows.

Consider any straight segment of plate for which the residual strain is assumed to vary linearly. By superposition, and the beam assumptions, the total strain will also vary linearly. Using the tri-linear stress-strain curve of Fig. 1, a linear variation of strain divides the plate segment into, at most, five regions, as shown in Fig. 11.

Let A and B designate the ends of the plate. When ε_A and ε_B are of the same sign, each may be in any one of the three strain ranges,

$$\varepsilon > \varepsilon_s \quad (21\text{-a})$$

$$\varepsilon_s > \varepsilon > \varepsilon_y \quad (21\text{-b})$$

$$\varepsilon_y > \varepsilon > 0 \quad (21\text{-c})$$

Hence there are nine possible combinations of regions, for the segment A-B, when ε_A and ε_B have the same sign. Similarly, there will be nine possible combinations when ε_A and ε_B are of opposite sign. When the strains ε_A and ε_B are known the normal stress and the tangent modulus is completely determined in each region of the plate segment, assuming no strain reversal.

To evaluate the tangent modulus section properties, one can modify the plate thickness in each region, by the modular ratio (see Fig. 11) and treat the transformed section as though it possessed a constant modulus. The determination of the instantaneous centroid, $\bar{C}$, the principal axes ξ and η, and the properties A^T, I_ξ^T and I_η^T is then straight forward.

In order to locate the instantaneous shear center, $\bar{S}$, relative to $\bar{C}$, let Fig. 12 represent an arbitrary transformed section and let $\bar{C}A$ be the initial radius from the origin of the transformed section co-ordinates X and Y. Sectorial area co-ordinates may be computed at the end points of each region by the relation

$$\omega_j = \omega_i + X_j Y_i - Y_j X_i \quad (22)$$

The sectorial static moment S_w, and the sectorial linear static moments S_{wX} and S_{wY} are defined (12) as

$$S_w = \int_A \omega dA \quad (23\text{-a})$$

$$S_{wX} = \int_A \omega Y dA \quad (23\text{-b})$$

$$S_{wY} = \int_A \omega X dA \quad (23\text{-c})$$

The co-ordinates of the shear center are then

$$X_{\bar{S}} = (S_{wX}\, I_Y - S_{wY}\, I_{XY})/(I_X\, I_Y - I_{XY}^2) \quad (24\text{-a})$$

$$Y_{\bar{s}} = -(S_{wY} I_X - S_{wX} I_{XY})/(I_X I_Y - I_{XY}^2) \qquad (24\text{-b})$$

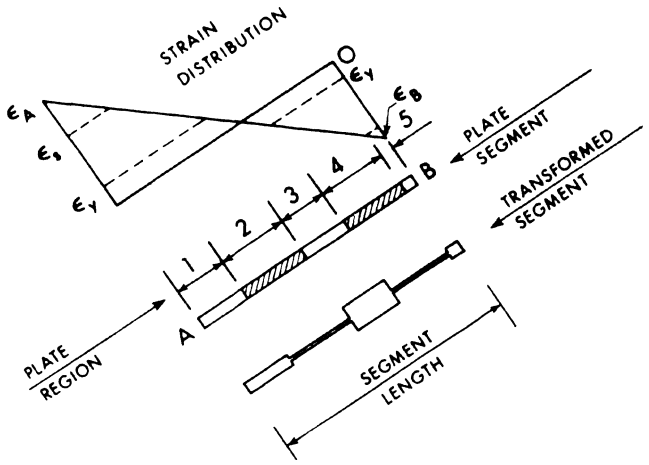

FIG. 11 Transformed Section of a Plate Segment

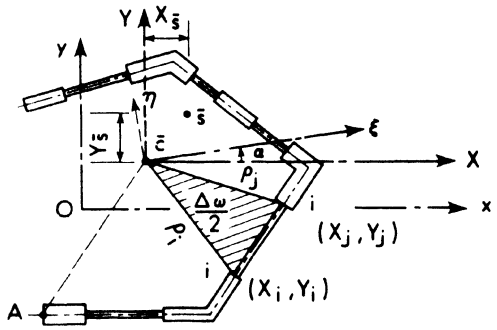

FIG. 12 Arbitrary Transformed Section

The sectorial area co-ordinates are now recomputed with $\bar{S}$ as the pole and $\bar{S}A$ as the initial radius.

The normalized warping co-ordinates, $\bar{\omega}$, may then be computed from the relation

$$\bar{\omega} = \omega_A - \left(\int_A \omega_A \, dA\right)/A \qquad (25)$$

and the section property $I_{w\zeta}$ is determined according to the definition (12)

$$I_{w\zeta} = \int_A \bar{\omega}^2 \, dA \qquad (26)$$

This is evaluated by the summation (see Fig. 12)

$$I_{w\zeta} = \sum_{k=1}^{n} \sum_{r=1}^{5} b_r t_r (\bar{\omega}_i^2 + \bar{\omega}_i\bar{\omega}_j + \bar{\omega}_j^2)/3 \qquad (27)$$

where r = the region of the plate segment and n = the number of plate segments.

Assuming G is proportional to E, St. Venant's torsional constant, J, may be computed by modifying the length of the region, rather than the width.

APPENDIX V - STRESS RESULTANTS

In carrying out Step 2 of the procedure to establish the strain distribution, it is necessary to evaluate P, M_x, M_y, and W_w with respect to C and S. For any given strain distribution, the plate segments are divided into regions as described in Appendix - IV and the stress resultants may be computed as

$$P \equiv \int_A \sigma_z \, dA = \sum_{k=1}^{n} \sum_{r=1}^{5} \frac{1}{2} b_r t_k (\sigma_{ir} + \sigma_{jr}) \qquad (28)$$

$$M_x \equiv \int_A \sigma_z \, y \, dA = \sum_{k=1}^{n} \sum_{r=1}^{5} \frac{b_r t_k}{6} [\sigma_{ir} (y_{jr} + 2y_{ir}) + \sigma_{jr} (y_{ir} + 2y_{jr})] \qquad (29)$$

$$M_y \equiv \int_A \sigma_z \, x \, dA = \sum_{k=1}^{n} \sum_{r=1}^{5} \frac{b_r t_k}{6} [\sigma_{ir} (x_{jr} + 2x_{ir}) + \sigma_{jr} (x_{ir} + 2x_{jr})] \qquad (30)$$

$$W_w \equiv \int_A \hat{\omega} \, \sigma_z \, dA = \sum_{k=1}^{n} \sum_{r=1}^{5} \frac{b_r t_k}{6} [\sigma_{ir} (\hat{\omega}_{jr} + 2\hat{\omega}_{ir}) + \sigma_{jr} (\hat{\omega}_{ir} + 2\hat{\omega}_{jr})] \qquad (31)$$

where r = plate region; n = number of plate segments; k = plate segment index; t_k = plate segment thickness; b_r = plate region length; and $\hat{\omega}$ = the normalized warping co-ordinate with respect to S.

To evaluate the geometric stiffness $[K_G]$ in Eq. 14 it is necessary to evaluate the stress resultants P, M_ξ, M_η, V_ξ, V_η, and $M_{\rho\zeta}$ which occur in Eq. 4. The stress resultant P is determined by Eq. 28. The stress resultants M_ξ and M_η are determined from the transformation

$$M_\xi = (M_x - Py_o) \cos\alpha - (M_y - Px_o) \sin\alpha \qquad (32\text{-a})$$

$$M_\eta = (M_y - Px_o) \cos\alpha + (M_x - Py_o) \sin\alpha \qquad (32\text{-b})$$

The quantity $M_{\rho\zeta}$ may be evaluated as

$$M_{\rho\zeta} = \sum_{k=1}^{n} \sum_{r=1}^{5} \frac{b_r t_k}{12} [\sigma_{ir}(4X_{ir}^2 + 2X_{jr}^2 + 4Y_{ir}^2 + 2Y_{jr}^2 - b_r^2) + \sigma_{jr} (4X_{jr}^2 + 2X_{ir}^2 + 4Y_{jr}^2 + 2Y_{ir}^2 - b_r^2)] \qquad (33)$$

In addition

$$V_\xi = (M_{\eta q} - M_{\eta p})/\ell \qquad (34\text{-a})$$

$$V_\eta = (M_{\xi q} - M_{\xi p})/\ell \qquad (34\text{-b})$$

where p and q are the node numbers of the element.

APPENDIX VI - ELEMENT MATRICES

Element matrices arise in Eq. 8, after substitution of Eqs. 5, 6, and 7 into Eq. 4 and integrating over the length of the element. The tangent stiffness, $[\bar{k}_s]$, arises from the terms

$$\int_\ell (\Delta P \, \delta w_\zeta - \Delta M_\xi \, \delta v_\eta'' - \Delta M_\eta \, \delta u_\xi'' + \Delta W_{w\zeta} \, \delta\phi'') d\ell \qquad (35)$$

and the geometric stiffness, $[\bar{k}_G]$, arises from the remaining terms with the exclusion of the loading terms.

After integration, expression 35 may be written symbolically as

$$\delta \langle \bar{\Delta r}_E \rangle [\bar{k}_s] \{\bar{\Delta r}_E\} \qquad (36)$$

where

$$[\bar{k}_s] = \begin{bmatrix} k_{uu} & & & \\ & k_{vv} & & \\ & & k_{\phi\phi} & \\ & & & k_{ww} \end{bmatrix} \tag{37}$$

and

$$\langle \bar{\Delta r}_E \rangle = \langle \{\underline{u}\}^T, \{\underline{v}\}^T, \{\underline{\phi}\}^T, \{\underline{w}\}^T \rangle , \tag{38}$$

the component nodal vectors being defined in Fig. 5.

The remaining terms evaluate as

$$\delta \langle \bar{\Delta r}_E \rangle [\bar{k}_G] \{\bar{\Delta r}_E\} \tag{39}$$

where

$$[\bar{k}_G] = \begin{bmatrix} g_{uu} & & g_{u\phi} & \\ & g_{vv} & g_{v\phi} & \\ g_{\phi u} & g_{\phi v} & g_{\phi\phi} & \\ & & & 0 \end{bmatrix} \tag{40}$$

Assuming A^T, I_ξ^T, I_η^T, P, M_ξ, M_η, $M_{\rho\zeta}$, e_ξ and e_η all vary linearly in the form

$$A^T = A_p^T + (A_q^T - A_p^T)\,\beta \tag{41}$$

where p and q are adjacent nodal numbers and β is the nondimensionalized co-ordinate of Fig. 5, the integrated matrices may all be written in terms of coefficient matrices of the form

$$[k_{st}^{nj}] = \int_0^1 \beta^j \{f_n^{(s)}\} \langle f_n^{(t)} \rangle \, d\beta \tag{42}$$

where n = the degree of the interpolation vector (see Eqs. 6); s and t indicate the order of differentiation; and j is the exponent of β. The numerical values of these matrices for specific values of s, t, n, and j are given in Table 1.

The matrices in Eqs. 37 and 40 then become

$$\frac{\ell^3}{E}[k_{uu}] = I^T_{\eta p}[k^{30}_{22}] + (I^T_{\eta q} - I^T_{\eta p})[k^{31}_{22}] \tag{43-a}$$

$$\frac{\ell^3}{E}[k_{vv}] = I^T_{\xi p}[k^{30}_{22}] + (I^T_{\xi q} - I^T_{\xi p})[k^{31}_{22}] \tag{43-b}$$

$$\frac{\ell^3}{E}[k_{\phi\phi}] = I^T_{w\zeta p}[k^{30}_{22}] + (I^T_{w\zeta q} - I^T_{w\zeta p})[k^{31}_{22}] \tag{43-c}$$

$$\frac{\ell}{E}[k_{ww}] = A^T_p[k^{20}_{11}] + (A^T_q - A^T_p)[k^{21}_{11}] \tag{43-d}$$

$$\ell[g_{uu}] = \ell[g_{vv}] = P_p[k^{30}_{11}] + (P_q - P_p)[k^{31}_{11}] \tag{43-e}$$

$$\ell[g_{u\phi}] = \ell[g_{\phi u}]^T = -V_\eta \ell[k^{30}_{10} + k^{31}_{11}] - M_{\xi p}[k^{30}_{11}] + P_p e_{\eta p}[k^{30}_{11}] + (P_q e_{\eta p} - 2P_p e_{\eta p} + P_p e_{\eta q})[k^{31}_{11}] + (P_q - P_p)(e_{\eta q} - e_{\eta p})[k^{32}_{11}] \tag{43-f}$$

$$\ell[g_{v\phi}] = \ell[g_{\phi v}]^T = V_\xi \ell[k^{30}_{10} + k^{31}_{11}] + M_{\eta p}[k^{30}_{11}] - P_p e_{\xi p}[k^{30}_{11}] - (P_q e_{\xi p} - 2P_p e_{\xi p} + P_p e_{\xi q})[k^{31}_{11}] - (P_q - P_p)(e_{\xi q} - e_{\xi p})[k^{32}_{11}] \tag{43-g}$$

$$\ell[g_{\phi\phi}] = GJ^*_p[k^{30}_{11}] + G(J^*_q - J^*_p)[k^{31}_{11}] \tag{43-h}$$

where $J^* = J + \frac{M_{\rho\zeta}}{G}$; (44)

J = the St. Venant torsion constant; and G = the shear modulus.

Prior to assembly, the element nodal displacement increments, $\{\bar{\Delta r}_E\}$, must be expressed in terms of displacement increments of the original reference points C and S. From the geometry of Fig. 4 we may write

$$u_\xi = u_s \cos\alpha + v_s \sin\alpha + \{(b_x - e_x)\sin\alpha - (b_y - e_y)\cos\alpha\}\,\phi \tag{45-a}$$

$$v_\eta = v_s \cos\alpha - u_s \sin\alpha + \{(b_y - e_y)\sin\alpha + (b_x - e_x)\cos\alpha\}\,\phi \tag{45-b}$$

$$w_\zeta = w_c - y_o v'_s - x_o u'_s \tag{45-c}$$

Evaluating displacements and displacement gradients at the nodes establishes the transformation matrix [T] of Eq. 9.

TABLE 1 - COEFFICIENT MATRICES

$$[k^{30}_{11}] = \begin{bmatrix} 36 & 3 & -36 & 3 \\ 3 & 4 & -3 & -1 \\ -36 & -3 & 36 & -3 \\ 3 & -1 & -3 & 4 \end{bmatrix} \qquad [k^{30}_{22}] = \begin{bmatrix} 12 & 6 & -12 & 6 \\ 6 & 4 & -6 & 2 \\ -12 & -6 & 12 & -6 \\ 6 & 2 & -6 & 4 \end{bmatrix}$$

$$[k^{31}_{11}] = \begin{bmatrix} 18 & 3 & -18 & 0 \\ 3 & 1 & -3 & -1/2 \\ -18 & -3 & 18 & 0 \\ 0 & -1/2 & 0 & 3 \end{bmatrix} \qquad [k^{31}_{22}] = \begin{bmatrix} 6 & 2 & -6 & 4 \\ 2 & 1 & -2 & 1 \\ -6 & -2 & 6 & -4 \\ 4 & 1 & -4 & 3 \end{bmatrix}$$

$$[k^{30}_{10}] = \begin{bmatrix} -15 & -3 & -15 & 3 \\ 3 & 0 & -3 & 1/2 \\ 15 & 3 & 15 & -3 \\ -3 & -1/2 & 3 & 0 \end{bmatrix} \qquad [k^{32}_{11}] = \begin{bmatrix} 72 & 15 & -72 & -6 \\ 15 & 4 & -15 & -3 \\ -72 & -15 & 72 & 6 \\ -6 & -3 & 6 & 18 \end{bmatrix}$$

$$[k^{20}_{11}] = \begin{bmatrix} 7 & -8 & 1 \\ -8 & 16 & -8 \\ 1 & -8 & 7 \end{bmatrix} \qquad [k^{21}_{11}] = \begin{bmatrix} 3 & -4 & 1 \\ -4 & 16 & -12 \\ 1 & -12 & 11 \end{bmatrix}$$